2009-01-01

Optical Properties of Silica-MFI Doped Acrylamide-based Photopolymer

Tzvetanka Babeva
Technological University Dublin

Rosen Todorov
Bulgarian Academy of Sciences

Svetlana Mintova
Laboratoire de Matériaux à Porosité Contrôlée, UMR-7016 CNRS

Temenujka Yovcheva
Plovdiv University

Izabela Naydenova
Technological University of Dublin, izabela.naydenova@tudublin.ie

Recommended Citation

Babeva, T. et al. (2009) Optical properties of silica MFI doped acrylamide-based photopolymer. *Journal of Optics A* Pure and Applied Optics, 11(2) 024015. doi:10.1088/1464-4258/11/2/024015

Optical properties of silica-MFI doped acrylamide-based photopolymer

T Babeva[1,2], R Todorov[2], S Mintova[3], T Yovcheva[4], I Naydenova[1] and V Toal[1,5]

[1] Centre for Industrial and Engineering Optics, Dublin Institute of Technology, Kevin Street, Dublin 8, Ireland

[2] Bulgarian Academy of Sciences, Central Laboratory of Photoprocesses, Acad. G. Bonchev Str., bl.109, 1113 Sofia, Bulgaria

[3] Laboratoire de Matériaux à Porosité Contrôlée, UMR-7016 CNRS, 68093 Mulhouse, France

[4] Plovdiv University, Department of Experimental Physics, 24 Tzar Assen str., 4000 Plovdiv, Bulgaria

[5] School of Physics, Dublin Institute of Technology, Kevin Street, Dublin 8, Ireland

E-mail: tzwetanka.babeva@student.dit.ie

Abstract

The optical properties of acrylamide-based photopolymer doped with pure silica MFI-type zeolites are studied by refractometric and spectrophotometric means. Dynamic Light Scattering and Transmission Electron Microscopy are used for zeolite characterization and laser refractometry and White Light Interferometric profilometry are used for surface characterization of the composites. Refractive indices and absorption coefficients of composites are determined from their transmittance and reflectance spectra. The calculated dispersion curves are further used for deriving the zeolites refractive index and porosity and the latter compared to the values of total pore volume obtained from N_2-sorption measurements. The impact of the doping level on the composite's optical properties both on the surface and in the volume are discussed.

Keywords: optical properties, photopolymer composites, zeolites, porosity, scattering.

PACS codes: 78.66.Sq, 82.35.Np, 78.67.Bf, 78.20.Ci, 78.20.Bh, 42.70.Jk, 07.60.Hv.

1.0 Introduction

The organic/inorganic nanocomposites are of great interest in advanced material science because they combine both the unique properties of the two constituents and may possess new properties not characteristic of the original components. In this way nanocomposites material exhibiting remarkable optical [1], mechanical [2,3], electrooptical [4], thermal [5] and electrical [6] properties can be obtained with a high potential for new applications [7,8]. Recently, controllable incorporation of solid nanoparticles such as SiO_2 [9,10], TiO_2 [11,12] and ZrO_2 [13] in holographic photopolymers opens up the opportunity for optimization, improvement and further development of recording capabilities of widely used photopolymers. It has been shown that at optimum values of recording intensity and volume fractions of incorporated nanoparticles a redistribution of particles occurs leading to an increase of diffraction efficiency of the recorded gratings due to a higher refractive index modulation [9-13]. The main issues arising in these hybrid systems are the compatibility between the polymer host and the dopants and the optical losses due to scattering that increases with the size of nanoparticles and the difference between the nanoparticle refractive index and that of the photopolymer matrix. To overcome these difficulties, small particles [13], or particles with organically modified shells [14,15] have been used. A different approach has been recently adopted in the Centre of Industrial an Engineering Optics at Dublin Institute of Technology where we use zeolites nanocrystals as dopants [16-18]. Zeolites are microporous crystalline material with uniform pore size distribution on the molecular scale and well defined ordered structure [19]. They are compatible with acrylamide photopolymer and layers with good optical quality are easy to produce [17]. Further, because their refractive index is relatively close to that of the photopolymer [20] the optical losses are acceptably low even in the case of bigger nanoparticles. An additional advantage of using zeolites as dopants is related to the possibility of controlling the pore shapes and sizes, hydrophilicity, hydrophobicity and overall particle size [21]. However, for optimizing the performance of zeolite nanocomposites, accurate knowledge of their properties is required. Understanding and predicting the influence of porosity and optical properties of each phase on the effective optical properties of the zeolite nanocomposites will benefit all applications, in particular holographic sensor design [22]. Moreover, it will be a clear advantage to develop a method for characterizing the refractive index of the zeolites when they are already incorporated in the photopolymer matrix because it is well known that the zeolite properties are strongly influenced by the possibility of zeolite pores to host different atoms.

In this paper we report studies of the effective optical properties of photopolymer nanocomposites consisting of an acrylamide–based photopolymer matrix embedded with pure

silica MFI-type (Si-MFI) zeolites in different weight concentrations. Laser refractometry utilizing the method of the disappearing diffraction pattern [23,24] operated at three wavelengths and White Light Interferometric Profilometry were used for surface characterization of the composites. Transmittance and reflectance spectra of nanocomposites were used for determination of the effective refractive indices and absorption coefficients of studied samples. The calculated optical properties were further used for determination of zeolite density and refractive index by the developed calculation procedure.

2.0. Experimental details

2.1 preparation and characterisation of pure silica MFI-type zeolite nanoparticles

Pure silica MFI particles (Si-MFI) with an average size of 70 nm were synthesized from a pre-hydrolyzed precursor solution having the following chemical composition: 7TPAOH: 25SiO_2: 1504H_2O: 100EtOH (the numbers are oxide ratios). The silica source used for preparation of the above solution was tetraethoxy silane (TEOS, Aldrich, 95 %) and the organic template was tetrapropylammonium hydroxide (TPAOH, Aldrich, 1M aqueous solution). After hydrothermal treatment of the precursor solution at 90°C for 48 hours, the Si-MFI crystals were purified in three steps of high-speed centrifugation (25000 rpm for 1 h) and redispersed in distilled water under ultrasonication. The nanocrystals were stabilized in the solution with a solid content of 5.0 wt.% and a pH of 9.5 and further used for doping of the acrylamide-based photopolymer. Figure 1 presents Dynamic Light Scattering measurements of the prepared zeolites.

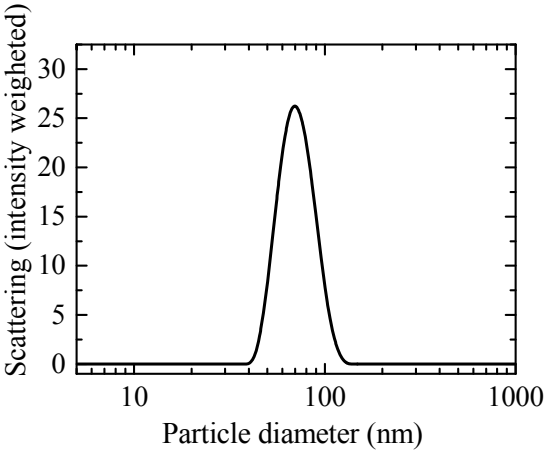

Figure 1. Dynamic Light scattering measurements of colloidal solution of Si-MFI zeolites (the mean hydrodynamic diameter is 70 nm)

It is seen that the mean hydrodynamic diameter of particles is 70 nm and the size dispersion is relatively low (the width of the half maximum is 15 nm). The size of the zeolite crystals is also confirmed by Transmission Electron Microscopy using a Philips CM 200 FEG operated at 200 kV. From the TEM image presented in figure 2 it can be seen that the particles are almost spherical in shape with physical size close to the hydrodynamic diameter.

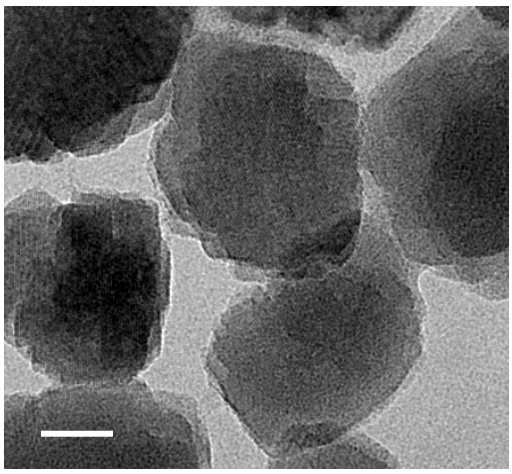

Figure 2. TEM images of pure silica MFI-type zeolites obtained at 200kV (the scale bar is 20 nm).

2.2. preparation and surface characterization of photopolymer nanocomposites

The photopolymer nanocomposite consists of a soft photopolymer matrix containing pure silica MFI-type (Si-MFI) zeolite nanoparticles. The standard photopolymer solution developed in Centre for Industrial and Engineering Optics-Dublin Institute of Technology [25] is used as a matrix. It consists of 9 ml stock solution of polyvinyl alcohol (20 w/w%), 2 ml triethanolamine, 0.6 g acrylamide, 0.2 g N,N-methylene bisacrylamide and 4 ml Erythrosin B dye of 1.1mM dye stock solution. The Si-MFI zeolites (5.0 wt.% H_2O colloidal solution) are added in concentrations from 0 to 7.0 wt.%. In order to obtain equal thicknesses of differently doped layers, distilled water is added to obtain a total volume of 50 ml. Amounts of 0.15 ml of the well mixed solution were gravity settled on levelled BK7 optical glass substrates with diameter of 2 cm, so the upper sides of the layers were open to the air. The thickness of the layers after drying for 24 h in darkness under normal laboratory conditions (t^{o} = (21 - 23) ^{o}C and RH = (40 - 60) %) was 30 ± 3μm. The dry layers were then exposed simultaneously to a UV and visible light (LV202 Megaelectronics) with intensity 2.5 mW/cm^2 for 30 min to achieve complete photopolymerisation.

The surface morphology of the nanocomposites was studied using a White Light Interferometric (WLI) surface profiler, MicroXAM S/N 8038, with vertical and lateral resolution of 1 nm and 1 μm, respectively. Figure 3 presents the surface images for undoped and 1, 3, 5 and 7 wt.% doped layers. The surface morphology for undoped layers is flat. With addition of nanoparticles it becomes roughened. It is seen that Si-MFI zeolites are distributed randomly on the surface and that there is a correlation between the doping level and height and density of particles on the surface. The increase of zeolite concentration in the layers leads to increase of peak heights and a decrease of the distance between them. Additional measurements of the surface roughness presented in figure 3(f) showed that root-mean-squared (rms) roughness increases from about 1 nm in the case of undoped layer to 7 nm for 7 wt% doped samples.

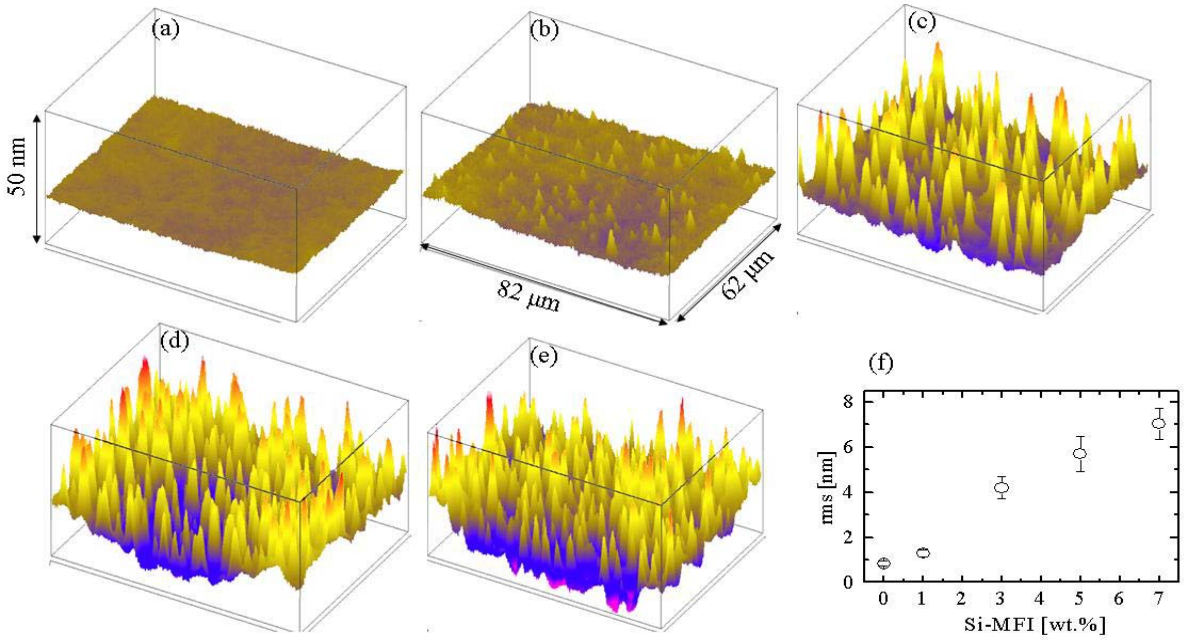

Figure 3. Surface profiles of undoped (a) and 1 wt% (b), 3wt% (c), 5 wt% (d) and 7 wt% (e) Si-MFI doped layers obtained using White Light Interferometric Surface profiler. Rms roughness as a function of doping level (f).

3.0 Results and discussions

3.1. Surface refractive index

Surface refractive indices of the layers, n_s, were measured at three wavelengths (406, 656 and 1320 nm) using a modified laser refractometer described in detail elsewhere [23,24]. Briefly

this refractometer is similar to the Abbe refractometer but one of the prisms is replaced by a diffraction grating [23,24]. In this case the value of the critical angle is determined as the angle at which the diffraction pattern disappears. The determination of refractive index of the layer is straightforward when the critical angle, refractive index and refracting angle of the prism are known. The error in n_s was estimated to be $\pm 1.10^{-3}$. It was determined by the accuracy with which the critical angle was measured and confirmed experimentally by measuring the refractive index of distilled water and comparing the obtained value with literature data [24]. Despite the fact that the penetration depth of the method has been estimated to be around 1μm [26] we use the term "surface refractive index" to distinguish these values from the volume values determined by spectrophotometric measurements.

Figure 4 presents the dependences of surface refractive index on zeolite concentration measured at three wavelengths. It is seen that the decrease in n_s with doping level is similar for the three wavelengths - 0.008 for 406 nm and 506 nm and 0.006 for 1320 nm.

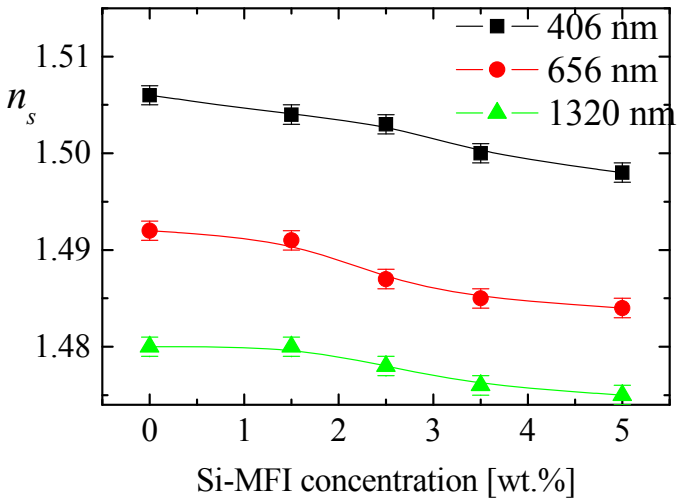

Figure 4. Surface refractive index as a function of Si-MFI concentration measured by laser refractometry at designated wavelengths: 406nm (■), 656nm (●) and 1320nm (▲).

Bearing in mind that the zeolite refractive indices (1.2-1.4 [20,27]) are less than that of the photopolymer (about 1.50 [28]) the observed decrease of n_s with increasing dopant concentration can be expected. However, if we regard the surface layer as an effective medium with different amounts of voids, its refractive index can be expected to decrease with increasing the voids (i.e roughness). Therefore it is difficult to draw a conclusion about the impact of doping level on the composite refractive index if only surface measurements are considered.

3.2. Volume refractive index

The next step in our investigation was determination of volume refractive index. We do not expect the surface roughness to have noticeable influence on the measured parameters because the contribution of the modified surface layer with thickness of about 50 nm (in the case of the highest zeolite concentration) is insignificant when the thickness of the investigated layer is about 30 μm.

Volume refractive indices of the photopolymer nanocomposites were determined by measuring transmittance, T and reflectances R_f and R_b from front (air) side and back (substrate) side of the layers, respectively using a high precision UV-VIS-NIR spectrophotometer, CARY 5E (VARIAN), with an accuracy of 0.1% in T and 0.5% in R. The simultaneous determination of refractive index, n, extinction coefficient, k and thickness, d of the layers was performed by minimization of the goal function F consisting of discrepancies between measured ("meas") and calculated ("calc") spectra:

$$F = \left(T_{calc} - T_{\mathrm{meas}}\right)^2 + \left(R_{fcalc} - R_{fmeas}\right)^2 + \left(R_{bcalc} - R_{bmeas}\right)^2 \tag{1}$$

F was minimized at each wavelength λ in the spectral range from 400-800 nm by a Nelder-Mead simplex method [29] using a dense grid of initial values of n, k and d.

In calculating T and R of the samples we assumed that the multiple transmitted and reflected waves at each boundary are incoherent and do not interfere with each other. In this case instead of summing their amplitudes we summed their intensities. Then T and R of a film positioned between two media (air and substrate) can be expressed by:

$$T = \frac{t_{af}\, t_{fs} \exp(-\alpha d)}{1 - r_{af}\, r_{fs} \exp(-2\alpha d)}; \quad R_f = r_{af} + \frac{t_{af}^2\, r_{fs} \exp(-2\alpha d)}{1 - r_{af}\, r_{fs} \exp(-2\alpha d)} \tag{2}$$

where $\alpha = 4\pi k/\lambda$ is the absorption coefficient in [cm^{-1}], t_{af} and t_{fs} are the transmitted intensities at air/film and film/substrates boundaries respectively and r_{af} and r_{fs} are the respective reflected intensities, that are functions of refractive indices of the two surrounding media-n_0 and n_{sub}, and of the complex refractive index of the layer $\bar{n} = n + ik$:

$$r_{af} = \left(\frac{n_0 - \bar{n}}{n_0 + \bar{n}}\right)\left(\frac{n_0 - \bar{n}}{n_0 + \bar{n}}\right)^*; \quad r_{fs} = \left(\frac{\bar{n} - n_{sub}}{\bar{n} + n_{sub}}\right)\left(\frac{\bar{n} - n_{sub}}{\bar{n} + n_{sub}}\right)^*; \quad t_{af} = 1 - r_{af}; \quad t_{fs} = 1 - r_{fs} \quad (3)$$

In eq. 3 the symbol (*) denotes the complex conjugate. The calculation of R_b is performed by substitution of n_0 by n_{sub} in the expression for r_{af} and n_{sub} by n_0 in the expression for r_{fs} (eq.3). The validation of this approach has been performed by high resolution measurements of T and R in the transparent range of the sample (λ > 600 nm) using very small wavelength steps (0.1 nm). The obtained spectra were free from interference peaks. If the multiple reflected and transmitted waves from upper and lower boundaries of the layer were coherent they would interfere and maxima and minima should appear in the measured spectra at wavelengths satisfying the condition [30]:

$$2nd = m\lambda, \quad (4)$$

where n and d are refractive index and thickness of the layer and m is an integer for maxima and a half-integer for minima. Simple estimations using eq. 4 showed that for n=1.45 and d=30 μm the wavelength separation for two consecutive maxima positioned around 800 nm (m=109 and 110) is 7.3 nm. Considering both that the measured spectra are interference free and that the wavelength resolution is sufficient to resolve peaks that are expected to be 7 nm apart, we can assume that the multiple reflected and transmitted waves do not interfere.

Figure 5 presents dispersion curves of refractive index and absorption coefficients for Si-MFI doped photopolymer calculated by minimization of the goal function F (eq.1). The errors in calculated values originating from errors in measured parameters (T and R) [31] are also shown. It is seen that the doping results in a decrease in n and an increase in α. As in the case of $n_{s,}$ considering that refractive index of zeolites is less than that of photopolymer, the decrease in n is expected.

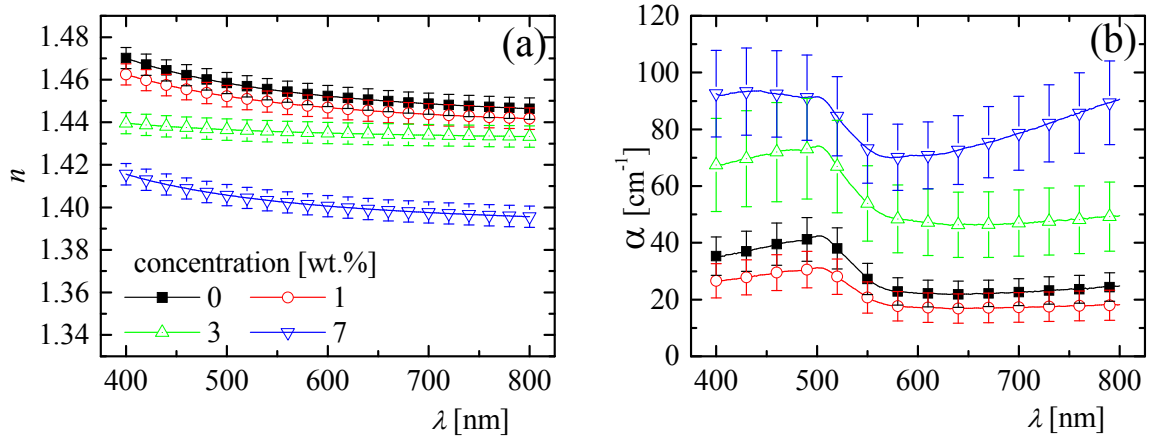

Figure 5. Dispersion curves of refractive index (a) and absorption coefficients (b) for Si-MFI doped photopolymer calculated by minimization of the goal function *F* (eq. 1).

The comparison between figure 4 and figure 5 shows that refractive index on the surface is higher than that in the volume and that the influence of doping is more pronounced in the volume (doping level of 7wt% leads to decrease in volume n by 0.05 but only by 0.008 in the surface refractive index). A possible reason for higher n_s could be that the zeolites are differently distributed through the volume and the surface layer is poorer in particles compared to the rest of the layer. But the difference between n_s and n exists for both doped and undoped layers. This leads us to assume that the most probable reason is that the surface dries faster than the volume and as a result the amount of residual water within is smaller leading to higher density and refractive index, respectively. Concerning the weaker influence of doping on the surface compared to the volume, we believe that the most probable reason is that some reactions take place on the surface. We expect that complementary confocal Raman spectroscopy investigations of the nanocomposite surface and volume which are in progress in our group will clarify further the reasons of different influence of particles on the surface and on the volume.

From figure 5(b) it is seen that absorption coefficient increases with doping level. The observed peak around 500 nm coincides with the peak in dye absorption, so we can assume that it is due to a small residual amount of dye in the layer. However, the general trend of slight increase in the optical losses is most probably due to the scattering rather than to absorption. To check this assumption we measured the diffuse reflectance of nanocomposites layers using an integrating sphere and a Spectralon® diffuse reflectance standard. The results are presented in Figure 6. For comparison the diffuse reflectance of the bare glass substrate is also shown.

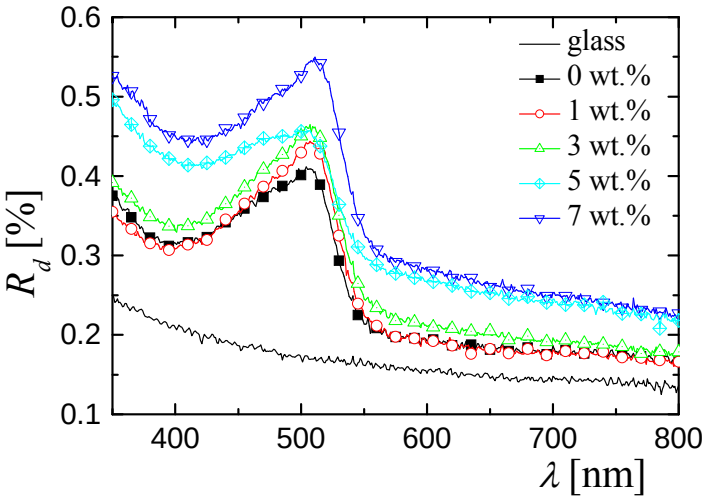

Figure 6. Diffuse reflectance of the Si-MFI doped photopolymers

The curves show similar trends - the reflectance increases both with decreasing wavelength and increasing doping level. The comparison with the spectrum of bare glass substrate shows that generally the layers are of good optical quality - the scattering is relatively small (about 0.5%) even for high concentration of the dopants.

3.3. Determination of zeolites' refractive index

For determination of zeolites' refractive index we used the Bruggeman effective medium theory [32]. The idea of all effective medium approximations is to regard the nanocomposites as a medium with effective properties that depend on the properties of the phases present and their volume fractions. In the case of two components medium (photopolymer and zeolite nanoparticles) the Bruggeman approximation has the form:

$$f_p \frac{\varepsilon_p - \varepsilon_e}{\varepsilon_p + 2\varepsilon_e} + f_z \frac{\varepsilon_z - \varepsilon_e}{\varepsilon_z + 2\varepsilon_e} = 0; \qquad f_p + f_z = 1, \tag{5}$$

where f_p and f_z are the respective volume fractions of photopolymer and zeolite particles and ε_p, ε_z and ε_e are the respective dielectric constants ($\varepsilon=n^2$) of photopolymer, nanoparticles and effective media. The two parameters ε_p and ε_e of eq.5 are already determined (ε_p and ε_e being the squared refractive index of undoped and differently doped samples, respectively) but there are still two unknown parameters (ε_z and f_z) and only one equation. Instead of using eq.5 at one wavelength we can use a system of similar equations at each wavelength in the spectral range 400-800 nm (for

example if the step is 5 nm the number of equations will be 81). However, in this case due to the expected dispersion of n_z (n_z is not a constant in the investigated spectral range) the number of unknowns also increases (the number of unknowns will be 82). To overcome this problem we used the Wemple-Di Domenico dispersion equation [33] for describing refractive index of the zeolites:

$$\varepsilon_z = n_z^2(E) = 1 + \frac{E_0 E_d}{E_0^2 - E^2}, \tag{6}$$

where E_0 and E_d are the so-called effective and dispersion energy, respectively and E is the light energy. In this way we limited the number of unknown to three (f_z, E_0 and E_d) keeping the same number of equations. The unknown parameters are determined through minimization of the goal function G (Eq. 7) using a non-linear subspace trust region method combining the interior-reflective Newton method with a preconditioned conjugate gradients method [34]:

$$G(f_z, E_d, E_0) = \sum_{i=1}^{81} \left\{ \frac{\varepsilon_p^i - \varepsilon_e^i}{\varepsilon_p^i + 2\varepsilon_e^i} + f_z \left(\frac{\varepsilon_z - \varepsilon_e^i}{\varepsilon_z + 2\varepsilon_e^i} - \frac{\varepsilon_p^i - \varepsilon_e^i}{\varepsilon_p^i + 2\varepsilon_e^i} \right) \right\}^2 \tag{7}$$

where ε_z as a function of E_0 and E_d (eq. 6) is used in eq. 7. For accurate and unambiguous minimization one needs proper initial values for the unknown parameters. Because such information is not available we used the following approach. The minimization procedure was run using a wide grid of initial values for the unknown parameters (E_0, E_d = 2 - 18 and f_z = 0 - 0.7) and the error function *Err* of the minimization was calculated as the residual value of the goal function at each solution:

$$Err = \sqrt{\sum_{i=1}^{81} \left| G(f_z, E_d, E_0) \right|^2}. \tag{8}$$

The dependence of *Err* on E_0 and E_d and its contour plot are shown in figure 7(a) and 7(b). It is seen that *Err* has a minimum value in the range E_d =7-10 eV and E_0 = 11.5-14 eV. In the next step we used these values as initial values and ran the minimization procedure again but using a narrower grid of initial values.

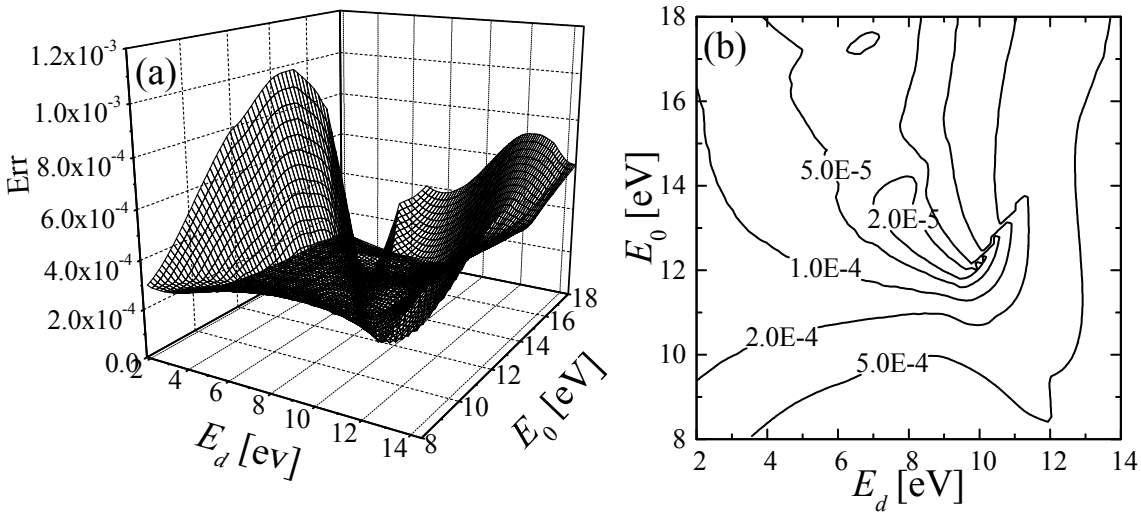

Figure 7. Three-dimensional (a) and contour (b) plots of the minimization error *Err*, calculated from eq. 8, as a function of E_0 and E_d.

The contour plot of error (eq.8) for the second minimization is shown in figure 8. It is seen that the solution with minimal errors can be found in the narrower range - $E_d \sim 9.5$ eV and $E_0 \sim 11.9$ eV. Note that the value of *Err* decreases by more than a factor of two when a finer grid of initial values is used.

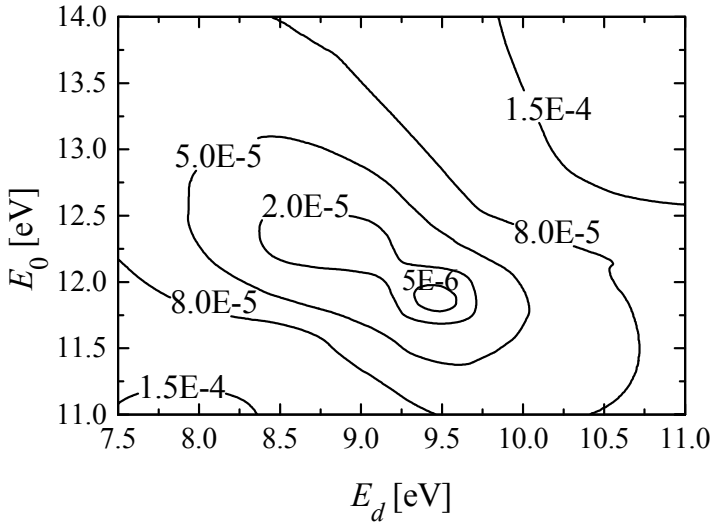

Figure 8. Contour plot of the error *Err* of minimization run with a narrow grid of initial values chosen from the area with lower error from the previous minimization.

In the final step the minimization was run with initial values of E_d = 9.5 eV, E_0 = 11.9 eV and f_z=0.01-0.7 and the final solution was chosen as the solution with minimal error. The *Err* value for the final solution was less than 10^{-7}.

Figure 9 presents the comparison between the calculated refractive index of Si-MFI zeolites (using the procedure described above) and the refractive index of amorphous SiO_2 [35]. The obtained values are in a good agreement with values obtained in the literature [27].

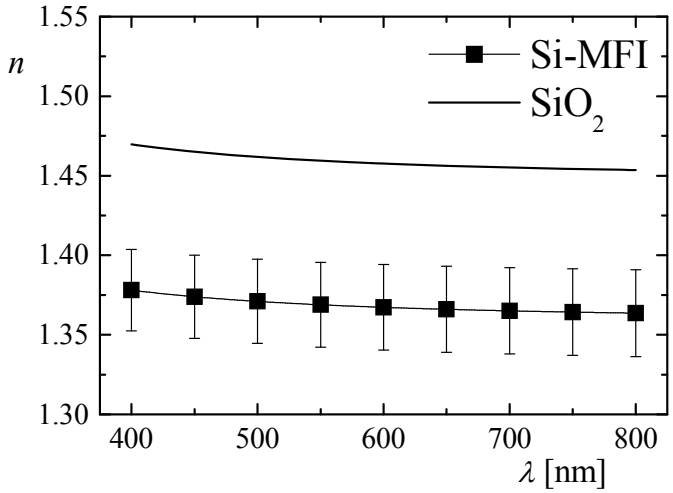

Figure 9. Comparison between refractive indices of pure silica MFI-type zeolites calculated using Bruggeman effective media approximation and the refractive index of amorphous silica [35]

If one regards the zeolites as an effective medium consisting of two phases – air and amorphous silica one can calculate the volume fraction of the two phases using the Bruggeman effective media approximation (Eq. 5). Further, when the volume fractions of air and silica are known one can determine the density of zeolites using literature data for silica density. The density of the zeolites phase ρ_z can be expressed as:

$$\rho_z = \frac{m_a + m_b}{V_a + V_b} = \frac{\rho_a V_a + \rho_b V_b}{V_a + V_b} = \rho_a \varphi_a + \rho_b \varphi_b \tag{9}$$

where m_a, ρ_a, V_a and m_b, ρ_b, V_b are the mass, density and volume of air and silica respectively and φ_a and φ_b are their volume fractions. The calculations give a value of 0.19 for φ_a and 0.81 for φ_b leading to a value of zeolite density of 1.78 g/cm^3 when the value of 2.2 g/cm^3 is used for SiO_2 density. We should note here that the theoretical calculation of MFI zeolites density based

on the frame work density leads to value of 1.76 g/cm^3 [36] which is in excellent agreement with the value calculated from refractive index data. Further considering that the densities of zeolites and silica are 1.78 g/cm^3 and 2.20 g/cm^3, respectively then 1g of each substance occupied 0.56 cm^3 and 0.45 cm^3. This means that the pore volume in zeolites can be estimated to be 0.11 cm^3/g. To validate the porosity values obtained by optical means N_2-sorption measurements (figure 10) have been conducted on thin layers prepared from zeolites using spin-coating deposition technique.

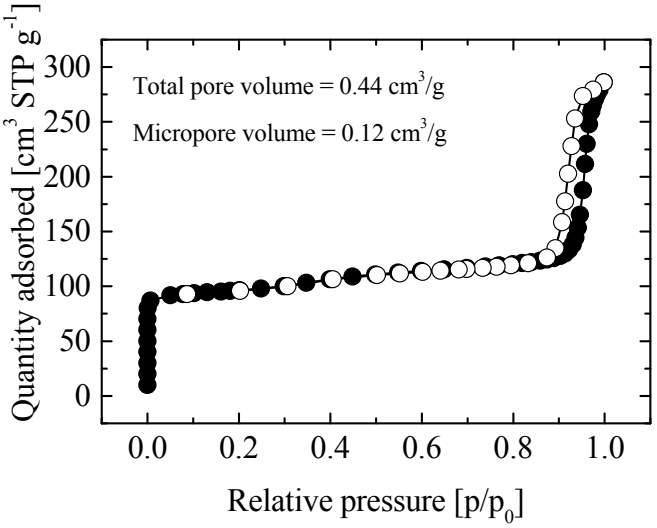

Figure 10. Nitrogen adsorption isotherms on Si-MFI zeolite thin films (open symbols denote desorption)

The rise of sorption at p/p_0 <0.05 corresponds to the filling of the micropores belonging to the zeolitic structures [37]. The small increase of amount adsorbed at relative pressure p/p_0 = 0.3-0.4 indicates the presence of mesopores. The hysteresis loop at p/p_0 > 0.6 is related to the capillary condensation in the inter-particle voids [37]. Using the calculation procedure described in detail elsewhere [37] a value of micropore volume of 0.12 cm^3/g was obtained. This value is in an excellent agreement with the value calculated from refractive index measurements (0.11 cm^3/g) when zeolites are considered as an effective medium consisting of SiO_2 and pores. Furthermore, this agreement showed that the pores of Si-MFI zeolite remain empty after the nanoparticles are added to the photopolymer mixture. This is consistent with the fact that the size of the pores is relatively small [36] and none of the organic components of the photopolymer are small enough to penetrate the openings and with the fact that the Si-MFI is hydrophobic [21] and the openings would not be filled with the water used as a solvent for the photopolymer.

The fact that the pores of the zeolites remain empty can be regarded as an advantage that favors the application of Si-MFI nanocomposites as medium for holographic recording. Otherwise, if the water enter the zeolites pores the zeolites refractive index would increase due to the replacement of air (n=1) with water (n=1.33). Consequently, when a redistribution of the nanoparticles is achieved, the refractive index modulation (the difference between the refractive index in areas rich of nanoparticles and areas with little or no nanoparticles present) will be smaller for the nanocomposites containing nanoparticles filled with water when compared with the nanocomposites containing empty pores nanoparticles. In the case of the filled with water nanoparticles in order to obtain the same difference in refractive index more zeolites should be incorporated in the photopolymer. This can lead to an increase of the optical losses due to scattering and may finally results in poor optical quality of the layers.

Conclusions

The optical properties (refractive index and absorption coefficient) of pure silica MFI doped acrylamide-based photopolymer were determined using refractometric and spectrophotometric measurements. It is found that the doping results in a decrease in refractive index both on the surface and in volume of the nanocomposites. The influence of doping is more pronounced in the volume of the composite than on the surface. A doping level of 7wt% leads to a decrease in refractive index of 0.05 (3.5 %) in the volume and 0.008 (0.5 %) on the surface. The observed increase in calculated absorption coefficients has been related to the optical losses due to scattering confirmed by diffuse reflectance measurements and root-mean-squared (rms) roughness measurements. The relatively small values of rms roughness (1nm for an undoped layer and 7 nm for a 7wt% doped layer) along with the small increase of diffuse reflectance for doped samples (0.5% in the case of heavily doped composites) indicate good optical quality of the nanocomposites.

A calculation procedure for deriving the zeolites refractive index and porosity/density has been developed. The Bruggeman effective media approximation is used both for zeolites refractive index calculation, regarding the nanocomposites as an effective medium of polymer and zeolites and for zeolite porosity determination when zeolites are regarded as an effective medium consisting of silica and pores. The microporosity of silica MFI zeolites calculated by optical means (0.11 cm^3/g) is in very good agreement with the micro pore volume calculated from N_2 sorption measurements (0.12 cm^3/g). The calculated density of Si-MFI zeolites (1.78 g/cm^3)

agrees very well with the theoretically calculated density based on framework density (1.76 g/cm^3).

Acknowledgements

This publication has emanated from research conducted with the financial support of Science Foundation Ireland grant N 065/RFP/PHY085 and COST Action MP0604.

The authors would like to acknowledge the School of Physics at DIT and Facility for Optical Characterisation and Spectroscopy, DIT for technical support.

T. Babeva would like to thank the Arnold F. Graves Postdoctoral programme at DIT.

References

[1] Sanchez C, Lebeau B, Chaput F and Boilot JP 2003 *Advanced Materials* **15** 1969

[2] Mammeri F, Le Bourhis E, Rozes L and Sanchez C 2005 *Journal of Materials Chemistry*, **15** 3787

[3] Jordan J, Jakobs K, Tannenbaum R, Sharaf M and Jasiuk I 2005 *Mat. Sci. & Eng. A* **393** 1

[4] Chapman R and Mulvaney P 2001 *Chem. Phys. Lett*. **349** 358.

[5] Yoon PJ, Fornes TD and Paul DR 2002 *Polymer* **43** 6727

[6] Gómez-Romero P, Chojak M, Cuentas-Gallegos K, Asensio JA, Kulesza PJ, Casañ-Pastor N and Lira-Cantú M 2003*Electrochemistry Communications* **5** 149

[7] Sanchez C, Julian B, Belleville P and Popall M 2005 *Journal of Materials Chemistry* **15** 3559

[8] Kickelbick G 2003 *Prog. Polym. Sci*. **28** 83

[9] Suzuki N and Tomita Y 2004 *Appl. Opt.* **43** 2125

[10] Tomita Y, Chikama K, Nohara Y, Suzuki N, Furushima K and Endoh Y 2006 *Opt. Letters* **31** 1402

[11] Suzuki N, Tomita Y, Kojima T 2002 *Appl. Phys. Lett*. **81** 4121

[12] Smirnova T, Sakhno O, Bezrodnyj V and Stumpe J 2005 *Applied Physics* **B80** 947

[13] Suzuki N, Tomita Y, Ohmori K, Hidaka M and Chikama K 2006 *Opt. Express* **14** 12712

[14] Kim W, Jeong Y and Park J 2005 *Appl. Phys. Letters* **87** 012106

[15] Sakhno O, Goldenberg L, Stumpe J and Smirnova T 2007 *Nanotechnology* **18** 105704

[16] Naydenova I, Sherif H, Mintova S, Martin S and Toal V 2006 *Proc. SPIE* **6252**

[17] Naydenova I and Toal V 2008 "Nanoparticle doped photopolymers for holographic applications" in *Ordered porous solids* Elsevier

[18] Ostrowski A, Naydenova I and Toal V 2008 paper submitted in *Journal of Optics A: Pure and Applied Optics*

[19] Mintova S, Valtchev V, Onfroy T, Marichal C, Knozinger H and Bein T 2006 *Microporous and Mesoporous Materials* **90** 237

[20] O. Larlus O, S. Mintova S, V. Valtchev V, B. Jean B, T. H. Metzger TH and T. Bein T 2004 *Applied Surface Science* **226** 155

[21] Eng-Poh Ng and Mintova S 2008 *Microporous and Mesoporous Materials* **114** 1

[22] I. Naydenova, R. Jallapuram, V. Toal and S. Martin 2008 Appl. Phys. Lett. **92** 031109

[23] Sainov S 1991 *Rev. Sci. Instr.* **62** 3106.

[24] Sainov S, Sarov Y and Kurtev S 2003 *Appl. Optics* **42** 2327.

[25] Martin S, Feely CA and Toal V 1997 *Appl. Opt*. **36** 5757

[26] Yovcheva T, Sainov S and Mekishev G 2007 *J. Optoelectron. Adv. Mater* **9** 2087

[27] Zhang J, Luo M, Xiao H and Dong J 2006 *Chem. Mater*. **18** 4

[28] Gallego S, Ortuño M, Neipp C, Márquez A, Beléndez A, Pascual I, Kelly JV and Sheridan JT 2005 *Opt. Express* **13** 3543

[29] Press W, Teukolsky S, Veterling W 1992 *Numerical recipes in C* (Cambridge University Press, 1992), Chap. 10, pp 408-410

[30] Swanepoel R 1983 *J. Phys. E: Sci. Instrum*. **16** 1214

[31] Konstantinov I, Babeva T and Kitova S 1998 *Appl. Opt*. **37** 4260

[32] Bruggeman DAG 1935 *Ann. Phys*. **24** 636

[33] Wemple SH and DiDomenico M 1971 *Phys. Rev. B* **3** 1338

[34] Coleman TF and Li Y 1996 *SIAM Journal on Optimization* **6** 418

[35] Paulick, *Handbook of Optical Constants of Solids*, (Academic Press, 1985)

[36] Baerlocher C, Meier WM and Olson DH 2001, *Atlas of Zeolite Framework Types*, Elsevier, Amsterdam, 2001.

[37] Prokesova-Fojtıkova P, Mintova S, Cejka J, Zilkova N and Zukal A 2006 *Microporous and Mesoporous Materials* **92** 154